Biogeosciences Discuss., 7, 387–428, 2010
www.biogeosciences-discuss.net/7/387/2010/

Biogeosciences
Discussions

This discussion paper is/has been under review for the journal Biogeosciences (BG).
Please refer to the corresponding final paper in BG if available.

Combined biogeophysical and biogeochemical effects of large-scale forest cover changes in the MPI earth system model

S. Bathiany[1,2], M. Claussen[1,3], V. Brovkin[1], T. Raddatz[1], and V. Gayler[1]

[1]Max Planck Institute for Meteorology, KlimaCampus, Hamburg, Germany
[2]School of Integrated Climate System Sciences, KlimaCampus, University of Hamburg, Germany
[3]Meteorological Institute, KlimaCampus, University of Hamburg, Germany

Received: 27 November 2009 – Accepted: 28 December 2009 – Published: 18 January 2010

Correspondence to: S. Bathiany (sebastian.bathiany@zmaw.de)

Published by Copernicus Publications on behalf of the European Geosciences Union.

Abstract

Afforestation and reforestation have become popular instruments of climate mitigation policy, as forests are known to store large quantities of carbon. However, they also modify the fluxes of energy, water and momentum at the land surface. Previous studies have shown that these biogeophysical effects can counteract the carbon drawdown and, in boreal latitudes, even overcompensate it due to large albedo differences between forest canopy and snow. This study investigates the role forest cover plays for global climate by conducting deforestation and afforestation experiments with the earth system model of the Max Planck Institute for Meteorology (MPI-ESM). Complete deforestation of the tropics (18.75° S–15° N) exerts a global warming of 0.4 °C due to an increase in CO_2 concentration by initially 60 ppm and a decrease in evapotranspiration in the deforested areas. In the northern latitudes (45° N–90° N), complete deforestation exerts a global cooling of 0.25 °C after 100 years, while afforestation leads to an equally large warming, despite the counteracting changes in CO_2 concentration. Earlier model studies are qualitatively confirmed by these findings. As the response of temperature as well as terrestrial carbon pools is not of equal sign at every land cell, considering forests as cooling in the tropics and warming in high latitudes seems to be true only for the spatial mean, but not on a local scale.

1 Introduction

As greenhouse gas concentrations are increasing rapidly, it is often discussed how carbon sinks can be generated in addition to emission reductions. In this regard, the terrestrial biosphere plays an important role. It is estimated to have stored about 166 Gt C (about 34% of total anthropogenic carbon) during the last two centuries, while total emissions of 200 Gt C are attributed to deforestation in this period (House, 2002). The Kyoto Protocol takes afforestation into account by considering such changes in carbon pools. As Pielke et al. (2002) point out, carbon has thus become the currency

to assess the human influence on global climate. However, the vegetation cover also affects important parameters of the land surface such as albedo, roughness length and hydrological properties (Nobre et al., 2004; Pielke et al., 1998). With few exceptions, the albedo of forest canopies is lower than the albedo of other vegetation or bare soil (Alton, 2009). Therefore, the net radiation at the surface tends to be larger which acts to increase near ground temperatures. In boreal latitudes, albedo differences are particularly large when snow is present, as the snow cover ~~is~~ partly masked by trees but not by herbaceous vegetation. In the tropics, the influence of forests on the water cycle is also important: Tropical forests are characterised by large evapotranspiration (ET) which acts to cool the surface. Due to deep roots, soil moisture can be returned to the atmosphere more efficiently (Nobre et al., 2004). In addition, trees increase the surface roughness, which leads to larger diffusive fluxes. Without further feedbacks, this would also lead to a cooling because the loss of energy has to be compensated by the surface net radiation. On the other hand, changes in wind speed and direction can lead to circulation changes (Sud et al., 1996), whose impact on temperature is less definite. Which mechanism prevails is a result of many nonlinear interactions and thus critically depends on the imposed changes and the original climate (Pitman et al., 2004). Moreover, these biogeophysical effects are linked to changes in the carbon cycle (biogeochemical effects) by several processes such as the dependence of transpiration on productivity and the dependence of plant physiology and structure on atmospheric CO_2 concentration (Betts et al., 1997).

Studies of the net effect of historical land cover change on global temperature have shown that biogeophysical and biogeochemical mechanisms are of the same order of magnitude (Matthews et al., 2004; Brovkin et al., 2006). Therefore, in order to quantifiy the impacts of large scale land cover changes appropriately, both effects should also be included. Claussen et al. (2001) used the intermediate complexity model CLIMBER-2 to implement a complete afforestation and deforestation in different latitude bands. A factor separation yielded a cooling biogeochemical, but a warming biogeophysical contribution of increased forest cover in each latitude. With combined effects they

found a temperature decrease (increase) resulting from afforestation (deforestation) in the tropics but the opposite effect in high northern latitudes. This result was confirmed by Bala et al. (2007), who applied a GCM with a coupled carbon cycle (INCCA). Betts (2000) used the radiative transfer model of HadAM3 to estimate the radiative forcing due to afforestation with conifer plantations in boreal latitudes. His geographically explicit calculation indicate that the masking of snow may not be the dominant mechanism everywhere, although on average a mean positive forcing was obtained. Other studies even challenge the warming influence of boreal forests for larger scales: Schaeffer et al. (2006) analysed the possibilities of extratropical afforestation based on socio-economically realistic scenarios for the 21st century. Their study demonstrates that the different time scales of biogeophysical and biogeochemical effects have to be considered. While the decrease in albedo dominates the temperature response in the first half of the century, global mean surface air temperature is reduced in 2100. Bird et al. (2008) developed a conceptual stand-based model and obtain a net cooling from year 40 on when the model is applied to several sites in Canada. As the main reason they identify the high cloud cover in spring which diminishes the surface forcing despite large albedo differences. Further objection is presented in Spracklen et al. (2008), who argue that the emission of cloud condensation nuclei from trees can cause a negative radiative forcing of several W/m^2 due to direct and indirect aerosol effects. Montenegro et al. (2009) used satellite observations to infer the potential net effect of small scale afforestation projects. They came to the conclusion that in all latitudes CO_2-sequestration is the dominating mechanism with a mean efficiency of 50%. Furthermore, no clear dependency on latitude was found. Considering these results, it seems definite that albedo differences counteract the carbon drawdown of afforestation in boreal latitudes and that biogeophysical effects should also not be neglected in other regions. However, the sign and amplitude of the global mean temperature response remains subject to many uncertainties.

In the following, the earth system model of the Max Planck Institute for Meteorology, MPI-ESM, is used to study the sensitivity of the coupled system to large scale

changes in forest cover. Apart from Bala et al. (2007), such an analysis has not yet been performed with a fully coupled AOGCM. In addition to the model differences, the longer integration time and the comparison to an anthropogenically undisturbed climate, this study differs from Bala et al. (2007) by considering afforestation as well as deforestation experiments, whereas biogeophysical and biogeochemical contributions are not calculated separately. Section 2 gives a short description of the model and the implementation of the experiments. Results are presented in Sect. 3 for global (Sect. 3.1) and regional changes of physical properties (Sect. 3.2) and carbon cycle effects (Sect. 3.3). In Sect. 4 these results are discussed with regard to previous studies of large-scale land cover changes, while final conclusions are drawn in Sect. 5.

2 Model and experiment setup

MPI-ESM consists of the atmosphere general circulation model ECHAM5 (Roeckner et al., 2003), the land surface model JSBACH (Raddatz et al., 2007), the ocean model MPIOM (Jungclaus et al., 2006) and the ocean biogeochemistry model HAMOCC5 (Maier-Reimer et al., 2005). ECHAM5 was run in T31 resolution (3.75°) with 19 vertical levels, MPIOM with approx. 3° and 40 vertical levels. JSBACH includes a dynamic vegetation module (Brovkin et al., 2009) which is based on a tiling approach. Within the vegetated fraction of each grid box 8 different plant functional types (PFTs) are considered: tropical and extratropical trees (both deciduous and evergreen), raingreen and cold shrubs, and C3- and C4-grasses. 7 pools of land carbon are distinguished in the model: a green pool, a reserve pool and a woody pool (the sum of these is referred to as living biomass), two litter pools and [illegible] soil pools. The photosynthesis scheme is based on Farquhar (1980) and for C4-grass on Collatz (1992). Soil respiration is calculated according to a Q_{10}-model and is linearly dependent on soil moisture, which is represented by a "bucket" approach. Physical land surface parameters such as albedo and roughness length are calculated from the individual properties of the PFTs and bare ground, weighted with their cover fractions for each land grid cell.

The equilibrium CO_2 concentration in the control run (CTL) amounts to 275 ppm. Orbital parameters were kept fixed at present day values and no anthropogenic land use was prescribed. Compared to observations, forest cover (Fig. 1) is distributed reasonably well in most parts of the globe (Brovkin, 2009). However, the equilibrium carbon storage (Fig. 2) differs from observations: In comparison with Prentice et al. (2001), the model underestimates vegetation carbon in boreal latitudes (2 kg/m^2 instead of 4–6 kg/m^2), while soil carbon is too large in Central and Eastern Asia. In the tropics, vegetation carbon seems to be better represented, while soil carbon pools of 20–40 kg/m^2 also exceed observations by a factor of 2.

Starting from this state, four 300 year experiments were conducted: tropical deforestation (DT), tropical afforestation (AT), boreal deforestation (DB) and boreal afforestation (AB). The term "tropical" here refers to the area between 18.75° S and 15° N, the "boreal" land cover change is applied between 45° N and 90° N. The latitudinal bands where chosen with regard to the distribution of forest PFTs in the model. In the deforestation cases, all PFTs but grass types were removed. In the afforestation cases, all PFTs but forest types were removed and the total vegetation cover was set to 1 in the areas under consideration except on ice shields. In all cases, the cover fractions of the remaining PFTs were then increased while keeping their relative composition fixed. In the case of boreal afforestation this procedure fails for grid cells, where no forest had previously existed. At these cells, deciduous and evergreen extratropical forest were taken with cover fractions of 50% each. As a result of the applied method, tree cover was expanded towards unproductive regions in the afforestation experiments. Since changes in biogeophysical parameters such as albedo and transpiration were calculated on a basis of changes in the carbon cycle, relative effects of afforestation are expected to be less than the deforestation effects. In all experiments, the new distribution of PFTs was kept fixed in the affected areas. For the other land cells, dynamic vegetation was still active.

The land cover change module of JSBACH was used to calculate the respective initial values of the carbon pools. Half of the vegetation carbon of the removed PFTs

was relocated to the atmosphere within the first year. The other half was immediately put into the soil pools. Carbon from litter and soil pools was transferred from removed tiles to expanded tiles. At the same time, the carbon densities of expanding tiles were reduced, so that there was no immediate carbon flux between these tiles and the atmosphere. As expected, the time scale of emissions is thus much faster than the time scale of sequestration, because plants have to accumulate carbon according to their productivity.

3 Results

3.1 Changes in global temperature and the carbon cycle

As a result of tropical deforestation, global mean temperature is increased by approx. 0.4 °C; the warming in high latitudes is particularly pronounced due to greenhouse forcing (Fig. 3). Because living carbon pools and forest cover are large in the tropics, the CO_2 increase of initially 60 ppm is much higher than in DB (Fig. 4). Changes in the ocean's carbon content are primarily a result of the CO_2-anomalies and not shown here; Fig. 5 depicts the changes in global terrestrial carbon. It is evident that DT is not only characterised by large primary emissions of approx. 123 Gt C due to biomass reduction, but also by net secondary emissions due to soil decomposition of almost the same amount. In fact, in the end of the experiment, tropical land cells contain 390 Gt C less than in CTL, of which the extratropical regions compensate 190 Gt C. During the first decades, the emissions from tropical soils are almost exactly balanced by the extratropical land and ocean sinks. This explains the constant CO_2 concentration in Fig. 4. As these sinks change on a larger time scale than the tropical land areas, they prevail after some 60 to 80 years and CO_2 concentration decreases. Around the year 90, extratropical land regions alone overcompensate the tropical sink, so that terrestrial carbon increases again.

In comparison to DT, terrestrial carbon pool anomalies are small in AT. Tropical land

areas take up approx. 0.33 Gt C/yr, decreasing atmospheric CO_2 by only 5 ppm within some decades. Thereafter, net emissions by the ocean and the extratropical biosphere are large enough to balance the tropical anomaly which approaches an equilibrium in the final century. Global mean temperature decreases by only 0.06 °C. Changes in AT are much smaller than in DT, because the converted area is smaller. Besides, climatic limitations play a role, as will be discussed in Sect. 3.3.

Things look quite different in the boreal experiments. In DB only approx. 20 Gt C are emitted instantaneously due to the ~~low~~ carbon storage of living biomass in boreal latitudes. The trend in global terrestrial carbon is close to zero because soil respiration in the cold regions is slow enough to be compensated by an enhanced productivity in the tropics. Therefore, the ocean uptake alone is responsible for the reduction of the CO_2-anomaly from 10 ppm to 3.7 ppm within the first 60 years. An additional reason for the slow response in the carbon pools of the deforested region is the large proportion of litter. Due to the experiment setup, litter is redistributed to expanding tiles and not put into the soil pools immediately. Because of the permanently increased litter flux during the first decades, soil carbon is first increased before it returns its original anomaly of +20 Gt C at the end of the experiment.

In the case of AB, extratropical as well as tropical regions exchange much more carbon than in AT. Large areas are available especially in the northern regions, so that 20 Gt C are stored in the first 15 years alone. CO_2-concentration is reduced by 5 ppm in this period, later the tropical and oceanic sources almost compensate the sequestration. While pools of living biomass and litter become saturated at +35 Gt C and +30 Gt C in the last decades, soil carbon increases almost linearly in the final 200 years and already contains 40 Gt C more than in CTL in the year 300. As the time scale of tropical soils is shorter, they compensate a considerable part of the boreal sink (more than 60 Gt C by the year 300), about twice as much as the ocean. Despite the CO_2 forcing, global mean temperature increases in AB (and decreases in DB) by approx. 0.25 °C. It is thus evident that biogeophysical mechanisms dominate the global mean temperature response in the boreal experiments.

3.2 Regional biogeophysical mechanisms

3.2.1 The tropical energy balance

Local temperature changes cannot be understood without analysis of the surface energy balance (Table 1). In DT a warming occurs despite of the increase in surface albedo. Without any feedbacks, this albedo increase would cause a reduction in net short-wave radiation by approx. $10\,W/m^2$. Instead, anomalies lie between -8 and $+8\,W/m^2$ because cloud cover is reduced by up to 0.06, with a mean of 0.028 over tropical land cells. Due to these compensating effects, the increased long-wave emission is the most important contribution to the decrease in net radiation at the surface. Because of warmer and drier conditions, the sensible heat flux is increased in DT, despite the reduced net radiation. The lack of energy is thus balanced by a strong reduction in ET.

Changes in AT are smaller than in DT and generally of opposite sign. However, two exceptions are apparent. Firstly, incoming long-wave radiation increases in both experiments. In AT, this is caused by increased cloud cover which overcompensates the reduced greenhouse effect. In DT, CO_2 forcing dominates and despite its decrease towards the end of the experiment, no qualitative changes in the energy balance occur over time (Table 1). The second difference between the experiments concerns the pattern of temperature changes. As Fig. 3 shows, cooling in AT does not take place at every individual land grid cell. In Northern Africa, the albedo difference amounts to up to 0.14 and net short-wave radiation is increased by $30\,W/m^2$. This is possible because of the large desert fraction in CTL at the northern boundary of the afforested region. Although ET and cloud cover are increased in Northern Africa, the albedo changes have the dominating influence on 2m-temperature. In Southern Africa cloud cover is not changed as uniformly as in other areas, so that in places with decreasing cloud cover and sufficient albedo changes, temperature does also increase. It is due to these warming regions, that the mean change in sensible heat flux is also positive.

3.2.2 Changes in the tropical water cycle

Apart from the exceptions mentioned in Sect. 3.2.1 it seems clear that the anomaly in ET is the main driver of temperature changes in the tropical land areas. This is corroborated by the changes in the annual cycle. Because of the seasonal shift of the ITCZ, precipitation mainly occurs in the summer of each hemisphere. Evaporation closely follows precipitation, while transpiration increases during the wet season when buckets are filled with water and stays high during the dry season until soil moisture becomes too small. In the dry period, transpiration contributes to total ET with more than 90%. In DT, temperature is particularly increased during the transition from the rainy to the dry season, when transpiration is reduced the most (Fig. 6 shows results for South America as an example). In addition, the reduction in ET leads to an increase in moisture convergence during March and August, which also dominates the annual mean. As a result, the positive soil moisture anomaly increases and shows the largest value during the moisture minimum after the dry season. In this time of the year, increased soil moisture can outweigh the reduced productivity of grass so that transpiration is equal or in some regions even higher than in CTL. The temperature increase is then probably only due to the elevated CO_2 concentration.

Table 2 summarises the annual mean changes in precipitation, ET and moisture convergence for different regions. In DT, the decrease in relative humidity and increase in surface albedo act to supress convection which explains the reduced precipitation. A large-scale sinking motion is induced in the mid-troposphere over most tropical land cells, while a rising anomaly occurs over the surrounding tropical oceans with exception of the South Atlantic. In AT, opposite changes are obtained. Table 2 also documents that changes in the centre of Amazonia are different from those in other regions. In central Amazonia, the reduction in precipitation is large enough to exceed that of ET, so that mean moisture convergence and soil moisture decrease. The precipitation decrease during the dry season (Fig. 6) is mostly attributable to this area. Also, ET is decreased in the second half of the year, so that the warming is even stronger during

this time, with up to 4 °C in September. The strong annual mean warming in central Amazonia which is evident in Fig. 3 is the result of these differences in the seasonal cycle. In contrast, the surrounding areas show an increase in soil moisture and moisture convergence as is shown in Fig. 7. While they dominate the spatial mean in DT, this is not the case in AT. Therefore, temperature in AT is mainly decreased (and soil moisture increased) in August and September. Because of the smaller size and the dryer climate of the afforested areas, changes in AT are much smaller than in DT.

3.2.3 The boreal energy balance

In the boreal experiments, temperature is mainly affected by albedo changes due to snow masking. The effect is strongest in spring when solar insolation is already large while snow cover is still high. As a result, land surface temperature anomalies are at a maximum during this season and reach 3 °C on zonal average. In DB, snow melt is delayed because of a lower spring temperature, while in AB it occurs earlier than in CTL (Fig. 8). The mean albedo anomaly is larger in AB than in DB, as snow cover and converted area in the northern parts are larger. It is due to the lower insolation that temperature does not change more than in the deforestation case. However, the temperature anomaly in AB stays large until summer, because snow melt occurs later in the north.

Due to the albedo changes the upwelling short-wave radiation is the largest contribution to the changes in net radiation (Table 1). In contrast to the tropics, the long-wave fluxes almost cancel each other. Annual mean changes in cloud cover are also low: DB shows a decrease by 0.003, AB an increase by only 0.001, which is both about one order of magnitude below the changes in the tropical experiments. However, annual mean short-wave insolation does change because of seasonal and spatial differences in cloud cover. In winter and spring, cloud cover is decreased by deforestation (in winter particularly at the southern edge of the affected area, so that it still exerts a radiative effect), in summer increased.

The cloud cover changes are in line with changes in the latent heat flux. In DB, the

growing season is delayed so that transpiration is reduced by approx. 0.15 mm/day in May. Evaporation is reduced by more than 0.1 mm/day in early spring because of lower temperatures. In summer and autumn, an increase in moisture convergence leads to higher soil moisture, so that ET hardly deviates from the control climate. This is in analogy to the situation at the end of the dry period in DT. Similar changes apply for AB but with opposite sign. Annually averaged sensible heat flux anomalies are smaller but of the same sign as the changes in latent heat flux. Outside the latitudes where land cover change was imposed, zonal mean changes in radiative and diffusive fluxes are small.

3.2.4 Sea ice and circulation feedbacks in boreal latitudes

The locally induced temperature changes are subject to feedbacks on a larger scale which concern sea-ice cover as well as the oceanic and atmospheric circulation. Although the changes in sea ice cover found here show large fluctuations, differences between the experiments are apparent: In DB, even in the Arctic Ocean the relative increase of sea ice cover is only 0.6% and not significant in most places in the years 101–300, although ice volume increases by 10.7% in this period. In the afforestation experiment, annual mean sea ice cover in the Arctic Ocean is decreased by 2.4% in the years 101–300 (1.65% in 151–300). The slightly stronger response in AB is most probably due to the fact that the largest albedo changes over land are located in more northern areas than in DB. The difference between DB and AB is most discernable in autumn (Fig. 9): Although the cooling over the Arctic Ocean in DB is stronger than over the adjacent land in most areas, the geographical pattern of the largest temperature anomalies resembles the short-wave forcing. This is not the case in AB, where the strongest warming occurs in proximity to the Arctic Ocean.

Changes in meridional overturning circulation (MOC) are more pronounced than those in sea ice cover. As Fig. 3 illustrates, the temperature response is weak and in some places even reversed in the north-western Atlantic in both experiments. In DB, the mass flux below 1000 m is increased by 1.5 Sv from 15.7 to 17.2 Sv at 30° N

on average over the final 200 years; in AB it is reduced by 1.5 Sv. At 60° N however, overturning is strongly enhanced in DB (from 5.7 Sv to 6.5 Sv), but hardly affected in AB (−0.1 Sv). This may be related to the decrease in ice cover in AB, so that larger buoyancy fluxes than in CTL are obtained.

The boreal land cover changes also influence atmospheric circulation. In DB the vertically extended cooling leads to an increase in baroclinity and thus in wind speeds in temperate northern latitudes, especially in spring. In 200 hPa, a zonal mean increase of up to 1 m/s is obtained. In contrast, high level wind speed in the subtropics is decreased in this season over the Atlantic and the Mediterranean. In AB, corresponding zonal mean anomalies are found. However, characteristic deviations from these zonal averages occur. The spatial heterogenity of the surface flux anomalies leads to barotropic Rossby wave patterns which show seasonal variations. In particular, an anticyclonic (cyclonic) anomaly occurs over Southeastern Europe in DB (AB) in spring which shifts to the east during the year. This shift indicates an interaction with a natural pattern: In CTL an anticyclone is simulated over the North Atlantic in spring (Azores high) which shows a similar shift and therefore seems to be extended to the east in DB and contracted in AB.

3.3 Regional changes in carbon pools

The climatic changes discussed above affect the local carbon pools. In addition, plant productivity is altered by the exchange of PFTs and changes in CO_2 concentration. Therefore, anomalies in total land carbon are not of the same sign everywhere in the tropical or boreal regions (Fig. 10). By rescaling the carbon pools of the individual tiles in CTL according to their altered cover fractions, the contributions of the PFT exchange alone can be obtained for each experiment. The difference to the actual changes is then due to climate and CO_2 feedbacks (neglecting all synergies). These feedbacks can be further separated by inferring changes in NPP and soil respiration with the same method. On the basis of this analysis, Fig. 10 can be interpreted in a more profound way: In the dry regions of Northern Australia and Northern Africa, as well as in the

north-east of South America, grass is simulated to be more productive than forest, so that deforestation leads to an increase and afforestation to a loss in soil carbon. In addition, the decreased moisture convergence in AT is accompanied by reduced soil moisture. As a result, total tropical soil carbon in AT decreases, despite the fact that more wood carbon tends to increase the turnover time. In the moist tropics, the increase (decrease) in soil moisture in DT (AT) acts to increase NPP with the exception of central Amazonia. Changes in soil moisture also have the largest impact on soil respiration in both experiments, so that respiration changes generally counteract the climatic effects on NPP. For example, in DT central Amazonia shows an increased turnover time even though the strongest warming occurs in this region. The extratropical sink in DT is due to CO_2-fertilisation, higher temperatures and, in some regions, a northerly shift of boreal forest. In the boreal areas simulated differences between grass and forest NPP are small in CTL. The very small amount of secondary emissions in DB is in line with this expectation; soil carbon has not at all contributed to secondary emissions by the year 300. In contrast to the tropics, the impact of temperature on NPP outweighs the effect of increased soil moisture except for the southern edge of the affected area in Central Asia. In AT, the reduced carbon storage of some land cells in Eastern Asia and Western North America is due to moisture induced soil respiration.

The spatial averages of carbon pools in and outside the areas of land cover change are presented in Table 3. For soil carbon, the feedback calculation explained above was applied. The separated impact of the redistribution of cover fractions is refered to as uncoupled. In DT, all contributions act to decrease the tropical carbon pools which explains the large secondary emissions in this experiment. The increased soil respiration overcompensates the enhanced productivity of grass in the tropics. However, in AT feedbacks also lead to a loss in soil carbon, because of increased soil respiration in Amazonia and larger water stress in other tropical areas. In addition to the low productivity differences, feedbacks are also responsible for the small emissions in DB. It has to be considered though, that soil carbon pools have not reached an equilibrium by the year 300 so that the absolute feedback contribution would further decrease in DB as

well as in AB.

As an afforestation project in reality will be most efficient in terms of carbon storage where a converted area has the strongest possible carbon uptake, the changes in carbon storage are also calculated with reference to the absolute afforested or deforested area only (Table 4). In the tropics, deforestation still has a much larger impact on carbon storage than afforestation because of the climatic limitations in the dry regions. In boreal areas, living biomass and litter are also less affected in AB than in DB. However, additional carbon is stored in the soil. It is evident that in AT and DB, where changes in soil carbon counteract the changes in biomass, the soil anomalies are smaller than in the corresponding experiments DT and AB. The difference between afforestation and deforestation illustrates, that for the whole area afforestation still leads to a gain and deforestation to a loss in soil carbon. Moreover, Table 4 documents that in all experiments the global mean anomalies are of the same sign as the immediate change in biomass, despite all productivity differences and feedbacks.

4 Discussion

4.1 Tropical experiments

Many GCM studies on the biogeophysical impact of large-scale deforestation in tropical regions have been conducted; a selection is presented in Table 5. Most of these studies show an increase in temperature and a decrease in ET and precipitation, which is in line with the results presented above. In addition, the large-scale sinking in response to the decrease in net energy at the surface is in accordance with expectations (Mylne and Rowntree, 1992; Dirmeyer and Shukla, 1994). The characteristic changes in surface energy balance and cloud cover also agree with CLIMBER-2 results (Ganopolski et al., 2001), with the exception that ~~downwellig~~ long-wave radiation is increased in DT due to CO_2 emissions. Changes in moisture convergence and the annual cycle of precipitation are less definite. For example, Nobre et al. (1991), Henderson-Sellers

et al. (1993), McGuffie et al. (1995) and Sud et al. (1996) find the largest decrease in Amazonian precipitation during the rainy season, whereas in DT the dry period is intensified in central Amazonia. The comparison with the studies listed in Table 5 is subject to many uncertainties which are introduced by the choice or calculation of surface parameter values (Mylne and Rowntree, 1992; Pitman et al., 1993; Dirmeyer and Shukla, 1994), the treatment of the ocean, different integration times and the definition of areas (McGuffie et al., 1995), as well as the applied model. In addition, no change in CO_2 concentration was accounted for in any of these experiments.

However, these differences may not explain why the changes in central Amazonia are much larger than elsewhere. By also using MPI-ESM, but without taking carbon cycle effects into account, Brovkin et al. (2009) find a similarly pronounced warming in Amazonia after global deforestation. Thus, these regional differences might rather be related to regional characteristics such as the amount of water recycling, which is known to be large in Amazonia (Nobre et al., 2004). For example, Pitman et al. (1993), McGuffie et al. (1995) and Zhang et al. (1996) also find the largest reduction of moisture convergence and the strongest (or only) temperature increase in Amazonia (Table 5). Sud et al. (1996) find a large warming and an exceptional decrease in moisture convergence in Amazonia as compared to the tropical mean. Also, Claussen et al. (2001) obtain the strongest warming in South America with CLIMBER-2.

In South East Asia, the water balance is less influenced by local recycling but rather by the monsoon circulation (Zhang et al., 1996). Changes in precipitation and ET are smaller than in Amazonia and the largest relative increase in moisture convergence after deforestation is obtained. In comparison to tropical Africa, absolute ET reduction in DT is larger while the temperature change is similar. The studies listed in Table 5 even report a cooling due to deforestation. Delire et al. (2001) obtained a reduction of SSTs due to increased upwelling. As CO_2 concentration is increased in DT, this cannot be expected here. However, a westward anomaly of ocean surface speed occurs during boreal spring and summer due to strengthened trade winds. The increase in SST is relatively low to the west of Indonesian land cells during this period.

In addition to these regional differences, the deforested continents may not be independent of each other. In Amazonia, the anomalies in moisture convergence (Fig. 7) hardly extend to the Pacific because of the Andes, as is also discussed by Lean and Rowntree (1997). In this regard it seems plausible that in Africa the anomalies can affect the nearby ocean more easily. In Fig. 7 a dipole structure is evident over the tropical Atlantic with more moisture convergence north and less moisture convergence south of the equator. This pattern is inherited by precipitation changes between July and October, which reflect a northerly shift of the ITCZ. Anomalies at the eastern boundary of South America could then propagate inland and add to the locally induced changes. However, to determine the extent to which the Amazonian climate is influenced by land cover changes in Africa further studies are needed.

4.2 Boreal experiments

With regard to the albedo induced cooling in spring and early summer, other GCM-studies of large scale boreal deforestation are qualitatively corroborated. Thomas and Rowntree (1992) as well as Chalita and LeTreut (1994) analysed the impact of albedo differences between closed snow cover and snow-covered forest. The temperature changes in MPI-ESM are similar to their results. Douville and Royer (1997) used the ARPEGE climate model and additionally considered the change in roughness length. They found a temperature maximum of more than 3 K in April and May between 50° N and 60° N, similar to MPI-ESM. However, the duration of the cooling is much less than reported by Douville and Royer: While they found a cooling of more than 2 K between December and June in the same latitudes, a comparable anomaly only persists for 3 months in MPI-ESM (Fig. 8). One reason might be the delayed snow melt in ARPEGE.

It must be considered though, that in all three studies there was no coupling between atmosphere and ocean. Bonan et al. (1992) and Ganopolski (2001) showed that if taking the ocean into account, the cooling is stronger, more evenly distributed over the year and geographically more extended. Bonan et al. (1992) found a cooling of locally

up to 5 K in July and 12 K in April. Snyder et al. (2004) obtained a cooling of 2.8 K (6.2 K in MAM) even with fixed SSTs because of a strong increase in low level cloudiness. As MPI-ESM includes the interaction with the ocean, the simulated temperature decrease in DB is much less than anticipated by comparison with other studies. The choice of replacement vegetation, changes in ET and the additional CO_2 of 5 ppm can not account for this difference. In contrast, large discrepancies to other models are apparent in the short-wave fluxes. Douville and Royer (1997) find a reduction of net short-wave radiation at the surface of more than 20 W/m^2 between 50° N and 65° N in March and April. In MPI-ESM the maximum value amounts to only 15 W/m^2. Bonan et al. (1995) and Thomas and Rowntree (1992) report an annual mean decrease in net radiation of 20–40 W/m^2, the latter 30–50 W/m^2 in April and May. Snyder et al. (2004) also found a decrease of 30 W/m^2 in MAM. As these values are generally averaged over different areas and time periods and represent different components of the surface radiative balance, the comparison cannot be perfectly consistent. However, it seems obvious that the sensitivity of the short-wave radiative balance to land cover change in high latitudes is comparatively weak in MPI-ESM. The reason seems to be related to the parameterisation of surface albedo: In comparison to observations from the BOREAS study, presented in Betts and Ball (1997), the albedo of snow-covered forests is too high in MPI-ESM. This is especially the case for deciduous forest, for which Betts and Ball find an albedo of 0.21, while in the model the values lie in the range of 0.4–0.7. For boreal evergreen forest, Betts and Ball state a mean of 0.13; in the model a range of 0.2–0.45 is found. Even in the boreal afforestation case, where maximal forest cover is assumed, albedo values are between 0.2 and 0.25. Also, measurements indicate that snow masking by deciduous and evergreen forest is similar (Betts and Ball, 1997; Robinson and Kukla, 1984). This is apparently not the case in MPI-ESM, although stems and branches are accounted for by a stem area index.

It seems plausible that the small change in sea ice cover in the boreal experiments is at least partly due to the weak temperature response in MPI-ESM. Ganopolski et al. (2001) found a 20% increase in global sea ice cover due to boreal deforestation in

CLIMBER-2. They also came to the conclusion that the thermal lag of the ocean and the ice-albedo feedback are the main reasons for a cooling in summer. This seems to be true for the autumn in AB, but not DB (Fig. 9). Results are not as distinct for the summer months. In contrast, the MOC increase of 1.5 Sv in DB agrees well with the 2 Sv obtained by Ganopolski et al. (2001). However, the diversity of model differences makes a causal assessment difficult. This also applies for atmospheric circulation changes. It is striking, that Douville and Royer (1997) also found a disturbance of the formation of the Azores High due to boreal deforestation. However, the similarities to their results are very limited, as Douville and Royer (1997) found a delayed rather than an earlier high. Also, they report weakened westerlies over Northern Europe and Russia, a southward shift of the North Atlantic westerly jet, increased surface pressure in high latitudes and reduced surface pressure over the mid-latitude Atlantic. All these features are of opposite sign in this study. A similarity can be found in the weakening of the Indian summer monsoon winds in DB, although this is not accompanied by a reduction in precipitation as in Douville and Royer (1997).

4.3 Global sensitivities

In order to assess the impact of forest cover changes independently of the area's size, Table 6 presents the sensitivity of global mean temperature and CO_2 content to changes in forest area. These are compared to Claussen et al. (2001) who present an analogue analysis for CLIMBER-2 in Fig. 1 of their study. The areas 10° N–20° N and 40° N–50° N in Claussen et al. (2001) are weighted only half here in order to account for the different choices of latitude bands.

Although CLIMBER-2 and MPI-ESM differ in many respects, the results are qualitatively similar. Nonetheless, with the exception of tropical deforestation, CO_2 sensitivities are smaller in MPI-ESM. In AT, the unproductive climate of dry regions prevents a larger CO_2 uptake, a feature that may not be as important in CLIMBER-2 because of the low resolution. In the case of boreal afforestation it must be considered that the carbon cycle had not yet reached a new equilibrium due to the shorter integration time.

The low CO_2-sensitivity of MPI-ESM to boreal deforestation is due to the low carbon storages of above ground biomass. However, this deficiency seems to be cancelled by the weak snow masking so that temperature sensitivities in high latitudes are similar in both studies. In the tropics, the differences in the sensitivity of temperature seem to reflect those in CO_2 content. As CO_2 concentration in DT is still decreasing in the year 300, sensitivities for this experiment are probably not well comparable.

In comparison to Bala et al. (2007), temperature changes are small in both deforestation experiments. The global warming of 0.7 K in the year 100 after tropical deforestation in Bala et al. (2007) may be related to larger carbon pools in INCCA. The corresponding CO_2 anomaly of 199 ppm is approx. 4 times larger than in MPI-ESM. In response to boreal deforestation, CO_2 anomalies are similar in both models, but albedo changes and thus global cooling are much more pronounced in INCCA. Nonetheless, the signs of global mean temperature changes obtained here are in line with the results of Bala et al. (2007), and for boreal latitudes also with Betts (2000). However, uncertainties remain concerning the role of individual processes. Claussen et al. (2001) as well as Bala et al. (2007) find a cooling biogeophysical contribution of tropical deforestation. The latter suggest that the albedo change dominates over the reduced ET in its impact on temperature because the ET of grass in INCCA is comparatively high. As the changes in tropical surface temperature and the energy balance demonstrate, this is not the case in MPI-ESM. Claussen et al. (2001) also obtain a warming at tropical land cells, even though it is counteracted on a global scale by the diminished greenhouse effect, resulting from reduced ET. In agreement with this, Ganopolski et al. (2001) report a warming over tropical land and a cooling over the oceans. As only coupled experiments have been conducted here, it cannot be determined whether this holds true for MPI-ESM.

5 Summary and conclusions

The experiments presented here show that in MPI-ESM forests tend to warm the surface in high northern latitudes but act to cool the surface in the tropics. Earlier model studies are corroborated by this result. A global temperature change of +0.4 °C and a CO_2 anomaly of initially 60 ppm is obtained after tropical deforestation because of large primary and secondary carbon emissions. In addition, the strong reduction in evapotranspiration leads to a pronounced warming in tropical land areas. While this is in line with the majority of biogeophysical GCM-studies, changes in the annual cycle and moisture convergence remain uncertain. For tropical afforestation, results are opposite to the deforestation experiment, but of much smaller magnitude, because productivity remains low in dry areas. CO_2 as well as global mean temperature are therefore hardly affected. In high latitudes the snow masking of trees in spring dominates the temperature response, although this effect is weaker than in other models. Changes in sea ice cover, meridional overturning in the ocean as well as atmospheric circulation modify the temperature anomalies, but the contribution of these feedbacks is also model dependent. Primary and secondary emissions are low in DB compared to DT because biomass pools and productivity differences between grass and trees are small. In the case of boreal afforestation, the large carbon sink is quickly cancelled by the ocean and tropical forests. CO_2 anomalies therefore do not exceed some ppm in both boreal experiments. Despite many model differences, the order of magnitude of global temperature and CO_2 sensitivities is similar to CLIMBER-2 results from Claussen et al. (2001).

For some land cells, a negative relation between forest cover and carbon storage is obtained, although they do not dominate the spatial mean in any experiment. Also, local temperature changes opposite to the global mean occur due to local differences in surface properties or feedbacks. This is mostly the case in Africa, where afforestation resulted in a warming in places with high surface albedo. Because of the dry conditions there, an afforestation would certainly not be feasible in reality. Nonetheless, as realistic

afforestation or reforestation projects must always be confined to much smaller areas than considered here, the spatial mean sensitivities do not apply in such cases. The magnitude and even the sign of biogeophysical and biogeochemical effects may then depend on the location. Therefore, studies such as Bird et al. (2008) and Montenegro et al. (2009), who challenge the idea of a warming boreal forest might be valid on a local scale and different from large-scale experiments.

In addition, many model limitations exist. In high latitudes, these primarily consist in the albedo of snow-covered forest. The representation of soil moisture as a single bucket neglects many important aspects such as the root depth of different plants. This may be particularly inadequate in the tropics, where changes in the water cycle are essential. As soil moisture has shown a large impact on productivity and soil respiration in the experiments, these uncertainties also affect the carbon cycle. In addition, neither the actual size of soil carbon pools nor the dependencies of NPP on temperature, soil moisture and atmospheric CO_2 as well as the dependency of soil respiration on temperature and moisture are constrained well and thus differ among models (Friedlingstein et al., 2006). As these mechanisms can act in opposite directions, the net effect on carbon pools may thus also be model dependent. In order to assess the impacts of forest cover changes in a more appropriate way, a better quantification of these effects from observations is therefore essential.

Acknowledgements. We would like to thank Hauke Schmidt for his useful comments. Also, Robert Schoetter is gratefully acknowledged for his lunchtime lessons.

The service charges for this open access publication
have been covered by the Max Planck Society.

References

Alton, P.: A simple retrieval of ground albedo and vegetation absorptance from MODIS satellite data for parameterisation of global land-surface models, Agr. Forest Meteorol., 149, 1769–

1775, 2009.
Bala, G., Caldeira, K., Wickett, M., Phillips, T. J., Lobell, D. B., Delire, C., and Mirin, A.: Combined climate and carbon-cycle effects of large-scale deforestation, P. Natl. Acad. Sci. USA, 104, 6550–6555, 2007.
Betts, A. K. and Ball, J. H.: Albedo over the boreal forest, J. Geophys. Res., 102, 28901–28909, 1997.
Betts, R. A., Cox, P. M., Lee, S. E., and Woodward, F. I.: Contrasting physiological and structural vegetation feedbacks in climate change simulations, Nature, 387, 796–799, 1997.
Betts, R. A.: Offset of the potential carbon sink from boreal forestation by decreases in surface albedo, Nature, 408, 187–190, 2000.
Bird, D. N., Kunda, M., Mayer, A., Schlamadinger, B., Canella, L., and Johnston, M.: Incorporating changes in albedo in estimating the climate mitigation benefits of land use change projects, Biogeosciences Discuss., 5, 1511–1543, 2008, http://www.biogeosciences-discuss.net/5/1511/2008/.
Bonan, G. B., Pollard, D., and Thompson, S. L.: Effects of boreal forest vegetation on global climate, Nature, 359, 716–718, 1992.
Bonan, G. B., Chapin III, F. S., and Thompson, S. L.: Boreal forest and tundra ecosystems as components of the climate system, Climatic Change, 29, 145–167, 1995
Brovkin, V., Claussen, M., Driesschaert, E., Fichefet, T., Kicklighter, D., Loutre, M. F., Matthews, H. D., Ramankutty, N., Schaeffer, M., and Sokolov, A.: Biogeophysical effects of historical land cover changes simulated by six earth system models of intermediate complexity, Clim. Dynam., 26, 587–600, 2006.
Brovkin, V., Raddatz, T., Reick, C. H., Claussen, M., and Gayler, V.: Global biogeophysical interactions between forest and climate, Geophys. Res. Lett., 36, L07405, doi:10.1029/2009GL037543, 2009.
Chalita, S. and Le Treut, H.: The albedo of temperate and boreal forest and the northern hemisphere climate: a sensitivity experiment using the LMD GCM, Clim. Dynam., 10, 231–240, 1994.
Claussen, M., Brovkin, V., and Ganopolski, A.: Biogeophysical versus biogeochemical feedbacks of large-scale land cover change, Geophys. Res. Lett., 28, 1011–1014, 2001.
Collatz, G. J., Ribas-Carbo, M., and Berry, J. A.: Coupled photosynthesis-stomatal conductance model for leaves of C4 plants, Aust. J. Plant Physiol., 19, 519–538, 1992.
Delire, C., Behling, P., Coe, M. T., Foley, J. A., Jacob, R., Kutzbach, J., Liu, Z., and Vavrus, S.:

Simulated response of the atmosphere-ocean system to deforestation in the Indonesian Archipelago, Geophys. Res. Lett., 28, 2081–2084, 2001.
Dirmeyer, P. A. and Shukla, J.: Albedo as a modulator of climate response to tropical deforestation, J. Geophys. Res., 99, 20863–20877, 1994.
Douville, H. and Royer, J.-F.: Influence of the temperate and boreal forests on the northern hemisphere climate in the Météo-France climate model, Clim. Dynam., 13, 57–74, 1997.
Farquhar, G. D., von Caemmerer, S., and Berry, J. A.: A biochemical model of photosynthetic CO_2 assimilation in leaves of C_3 species, Planta, 149, 78–90, 1980.
Friedlingstein, P., Cox, P., Betts, R., Bopp, L., von Bloh, W., Brovkin, V., Cadule, P., Doney, S., Eby, M., Fung, I., Bala, G., John, J., Jones, C., Joss, F., Kato, T., Kawamiya, M., Knorr, W., Lindsay, K., Matthews, H. D., Raddatz, T., Rayner, P., Reick, C., Roeckner, E., Schnitzler, K.-G., Schnur, R., Strassmann, K., Weaver, A. J., Yoshikawa, C., and Zeng, N.: Climate-carbon cycle feedback analysis: Results from the C4MIP model intercomparison, J. Climate, 19, 3337–3353, 2006.
Ganopolski, A., Petoukhov, V., Rahmstorf, S., Brovkin, V., Claussen, M., Eliseev, A., and Kubatzki, C.: CLIMBER-2: a climate system model of intermediate complexity. Part II: model sensitivity, Clim. Dynam., 17, 735–751, 2001.
Henderson-Sellers, A., Dickinson, R. E., Durbidge, T. B., Kennedy, P. J., McGuffie, K., and Pitman, A. J.: Tropical deforestation: Modeling local- to regional-scale climate change, J. Geophys. Res., 98, 7289–7315, 1993.
House, J. I., Prentice, I. C., and Le Quere, C.: Maximum impacts of future reforestation or deforestation on atmospheric CO_2, Glob. Change Biol., 8, 1047–1052, 2002.
Jungclaus, J. H., Keenlyside, N., Botzet, M., Haak, H., Luo, J.-J., Latif, M., Marotzke, J., Mikolajewicz, U., and Roeckner, E.: Ocean circulation and tropical variability in the coupled model ECHAM5/MPI-OM, J. Climate, 19, 3952–3972, 2006.
Lean, J. and Rowntree, P. R.: Understanding the sensitivity of a GCM simulation of Amazonian deforestation to the specification of vegetation and soil characteristics, J. Climate, 10, 1216–1235, 1997.
Maier-Reimer, E., Kriest, I., Segschneider, J., and Wetzel, P.: The HAMburg Ocean Carbon Cycle model HAMOCC 5.1 – Technical description, Release 1.1, Technical report 14/2005, Max-Planck Institute for Meteorology, Hamburg, 2005.
Matthews, H. D., Weaver, A. J., Meissner, K. J., Gillet, N. P., and Eby, M.: Natural and anthropogenic climate change: Incorporating historical land cover change, vegetation dynamics

and the global carbon cycle, Clim. Dynam., 22, 461–479, 2004.
McGuffie, K., Henderson-Sellers, A., Zhang, H., Durbridge, T. B., and Pitman, A. J.: Global climate sensitivity to tropical deforestation, Global Planet. Change, 10, 97–128, 1995.
Montenegro, A., Eby, M., Mu, Q., Mulligan, M., Weaver, A. J., Wiebe, E. C., and Zhao, M.: The net carbon drawdown of small scale afforestation from satellite observations, Global Planet. Change, 69, 195–204, 2009.
Mylne, M. F. and Rowntree, P. R.: Modelling the effects of albedo change associated with tropical deforestation, Climatic Change, 21, 317–343, 1992.
Nobre, C. A., Sellers, P. J., and Shukla, J.: Amazonian deforestation and regional climate change, J. Climate, 4, 957–988, 1991.
Nobre, C. A., Silva Dias, M. A., Culf, A. D., Polcher, J., Gash, J. H. C., Marengo, J. A., and Avissar, R.: The Amazonian climate, in: Vegetation, Water, Humans and the Climate: A New Perspective on an Interactive System, Springer, Berlin, Heidelberg, 79–92, 2004.
Pielke Sr., R. A., Avissar, R., Raupach, M., Dolman, A. J., Zeng, X., and Denning, A. S.: Interactions between the atmosphere and terrestrial ecosystems: influence on weather and climate, Glob. Change Biol., 4, 461–475, 1998.
Pielke Sr., R. A., Marland, G., Betts, R. A., Chase, T. N., Eastman, J. L., Niles, J. O., Niyogi, D. S., and Running, S. W.: The influence of land-use change and landscape dynamics on the climate system: relevance to climate-change policy beyond the radiative effect of greenhouse gases, Philos. T. R. Soc. Lond., 360, 1705–1719, 2002.
Pitman, A. J., Durbridge, T. B., Henderson-Sellers, A., and McGuffie, K.: Assessing climate model sensitivity to prescribed deforested landscapes, Int. J. Climatol., 13, 879–898, 1993.
Pitman, A. J., Dolman, H., Kruijt, B., Valentini, R., and Baldocchini, D.: The climate near the ground, in: Vegetation, Water, Humans and the Climate: A New Perspective on an Interactive System, Springer, Berlin, Heidelberg, 9–19, 2004.
Polcher, J. and Laval, K.: The impact of African and Amazonian deforestation on tropical climate, J. Hydrol., 155, 389–405, 1994a.
Polcher, J. and Laval, K.: A statistical study of the regional impact of deforestation on climate in the LMD GCM, Clim. Dynam., 10, 205–219, 1994b.
Prentice, I., Farquhar, G., Fasham, M., Goulden, M., Heimann, M., Jaramillo, V., Kheshgi, H., Le Quere, C., Scholes, R., and Wallace, D.: The carbon cycle and atmospheric carbon dioxide, in: Climate Change 2001: The Scientific Basis. Contribution of Working Group I to the Third Assessment Report of the Intergovernmental Panel on Climate Change, edited by:

Houghton, J. T., Ding, Y., Griggs, D. J., Noguer, M., van der Linden, P., Dai, X., Maskell, K., and Johnson, C. I., Cambridge University Press, Cambridge, 183–237, 2001.
Raddatz, T. J., Reick, C. H., Knorr, W., Kattge, J., Roeckner, E., Schnur, R., Schnitzler, K.-G., Wetzel, P., and Jungclaus, J.: Will the tropical land biosphere dominate the climate-carbon cycle feedback during the twenty-first century?, Clim. Dynam., 29, 565–574, 2007.
Robinson, D. A. and Kukla, G.: Albedo of a dissipating snow cover, J. Clim. Appl. Meteorol., 23, 1626–1634, 1984.
Roeckner, E., Baeuml, G., Bonaventura, L., Brokopf, R., Esch, M., Giorgetta, M., Hagemann, S., Kirchner, I., Kornblueh, L., Manzini, E., Rhodin, A., Schlese, U., Schulzweida, U., and Tompkins, A.: The atmospheric general circulation model ECHAM5. Part I: Model description, Max-Planck Institute for Meteorology, Report 349, 2003.
Schaeffer, M., Eickhout, B., Hoogwijk, M., Strengers, B., van Vuuren, D., Leemans, R., and Opsteegh, T.: CO_2 and albedo climate impacts of extratropical carbon and biomass plantations, Global Biogeochem. Cy., 20, GB2020, doi:10.1029/2005GB002581, 2006.
Snyder, P. K., Delire, C., and Foley, J. A.: Evaluating the influence of different vegetation biomes on the global climate, Clim. Dynam., 23, 279–302, 2004.
Spracklen, D. V., Bonn, B., and Carslaw, K. S.: Boreal forests, aerosols and the impacts on clouds and climate, Philos. T. R. Soc. A, 366, 4613–4626, 2008.
Sud, Y. C., Walker, G. K., Kim, J.-H., Liston, G. E., Sellers, P. J., and Lau, W. K.-M.: Biogeophysical consequences of a tropical deforestation scenario: a GCM simulation study, J. Climate, 9, 3225–3247, 1996.
Thomas, G. and Rowntree, P. R.: The boreal forests and climate, Q. J. Roy. Meteor. Soc., 118, 469–497, 1992.
Zhang, H., Henderson-Sellers, A., and McGuffie, K.: Impacts of tropical deforestation. Part I: Process analysis of local climatic change, J. Climate, 9, 1497–1517, 1996.

Table 1. The surface energy balance averaged over tropical and boreal land cells. Values for the experiments are given as deviations from the control climate. All fluxes are in W/m^2, surface temperature in °C. For DT, the time periods 11–60 and 271–300 have been considered separately, all other runs are averaged over the years 11–300. α_{surf}=surface albedo, α_{TOA}=top of atmosphere albedo, SW=short-wave, LW=long-wave, Rn=net radiation, SH=sensible heat flux, LH=latent heat flux, T_{surf}=surface temperature.

	Tropics (18.75° S–15° N)				Boreal (45° N–90° N)			Boreal, MAM		
	CTL	ΔDT yr 11–60	ΔDT yr 271–300	ΔAT	CTL	ΔDB	ΔAB	CTL	ΔDB	ΔAB
α_{surf}	0.159	+0.042	+0.042	−0.017	0.269	+0.070	−0.075	0.350	+0.107	−0.128
α_{TOA}	0.316	+0.004	+0.007	−0.003	0.471	+0.017	−0.018	0.493	+0.023	−0.023
SW↓	215.5	+8.1	+6.7	−2.7	96.9	+3.4	−2.9	134.4	+11.2	−11.5
SW↑	34.2	+10.8	+10.4	−4.1	26.1	+8.0	−7.8	47.0	+19.4	−19.7
net SW	181.3	−2.6	−3.7	+1.4	70.8	−4.6	+4.9	87.4	−8.2	+8.2
LW↓	390.4	+3.0	+1.9	+0.4	267.0	−4.1	+4.4	261.7	−7.6	+6.5
LW↑	453.3	+7.5	+5.5	−0.7	305.1	−4.8	+5.2	299.7	−7.9	+6.9
net LW	−62.9	−4.5	−3.6	+1.1	−38.1	+0.6	−0.9	−38.0	+0.3	−0.4
Rn	118.4	−7.1	−7.3	+2.5	32.7	−3.9	+4.0	49.4	−7.9	+7.8
SH	39.3	+2.7	+1.4	+0.4	8.2	−1.7	+1.6	15.7	−2.6	+3.1
LH	79.1	−9.8	−8.7	+2.0	22.6	−2.3	+2.4	23.6	−4.9	+4.4
T_{surf}	25.8	+1.2	+0.9	−0.1	−3.7	−1.1	+1.2	−4.5	−1.9	+1.7

Table 2. Changes in surface temperature (T), precipitation (P), evapotranspiration (ET) and moisture convergence (P-ET) in the Amazon (Am), central Amazon (Am-cent), tropical Africa (Af), Southeastern Asia (SEA) and the whole tropics (Trop) in the years 11–300. Am-cent consists of 8 grid cells with the boundaries 73° W, 58° W, 7.5° S and the equator.

Area and experiment	ΔT [K]	ΔP [mm/yr]	ΔET [mm/yr]	Δ(P-ET) [mm/yr]
Am (DT)	+1.6	−138 (9.2%)	−160 (13.3%)	+22 (7.5%)
Am (AT)	−0.2	+44 (3.0%)	+29 (2.5%)	+15 (5.1%)
Am-cent (DT)	+3.4	−467 (25.1%)	−342 (22.5%)	−124 (37.1%)
Am-cent (AT)	−0.4	+79 (4.3%)	+32 (2.1%)	+47 (14.0%)
Af (DT)	+1.0	−75 (8.2%)	−87 (10.9%)	+12 (10.4%)
Af (AT)	−0.1	+27 (3.0%)	+24 (3.0%)	+3 (2.9%)
SEA (DT)	+1.0	−107 (8.5%)	−135 (12.2%)	+28 (17.7%)
SEA (AT)	−0.1	+20 (1.6%)	+23 (2.1%)	−3 (1.8%)
Trop (DT)	+1.2	−104 (8.7%)	−122 (12.2%)	+18 (9.5%)
Trop (AT)	−0.1	+33 (2.8%)	+26 (2.6%)	+7 (3.7%)

Table 3. Anomalies of terrestrial carbon storage in kg/m^2, averaged over the manipulated latitude bands and the final 10 years of each experiment (ice sheets not included).

Area	Pools	DT	AT	DB	AB
Directly affected latitudes	Total	−11.71	+1.41	−1.43	+2.71
	Living biomass and litter	−8.60	+1.75	−1.88	+1.70
	Soil (uncoupled)	−2.46	+1.24	+0.33	+1.38
	Soil (feedbacks only)	−0.64	−1.58	+0.12	−0.37
Other land areas	Total	+1.74	−0.20	+0.42	−0.68
	Living biomass and litter	+0.27	−0.01	+0.12	−0.07
	Soil	+1.47	−0.19	+0.30	−0.61
Global	Total	−1.51	+0.19	−0.15	+0.37
	Living biomass and litter	−1.87	+0.42	−0.50	+0.48
	Soil (uncoupled)	−0.60	+0.30	+0.10	+0.43
	Soil (feedbacks only)	+0.96	−0.53	+0.24	−0.54

Table 4. Anomalies of terrestrial carbon storage in kg/m^2, averaged over the area of exchanged PFTs and the final 10 years of each experiment (ice sheets not included).

Pools	DT	AT	AT-DT	DB	AB	AB-DB
Total	−16.66	4.39	21.05	−3.06	4.46	7.52
Living biomass and litter	−12.23	5.45	17.68	−4.02	2.80	6.82
Soil (uncoupled)	−3.5	3.86	7.36	0.71	2.27	1.56
Soil (feedbacks only)	−0.91	−4.92	−4.01	0.06	−0.61	−0.67
Soil, total	−4.41	−1.06	3.35	0.77	1.66	0.89

Table 5. Changes in surface temperature (T), precipitation (P), evapotranspiration (ET) and moisture convergence (P-ET) in Amazonia (Am), tropical Africa (Af), Indonesia (In), South-eastern Asia (SEA) and the whole tropics (Trop) in previous (biogeophysical) model studies of large-scale deforestation. Zhang et al. (1996) refer to surface air temperature instead of ground surface temperature. In Pitman et al. (1993) this information is not definite.

Publication	Area	Remarks	ΔT [K]	ΔP [mm/yr]	ΔET [mm/yr]	$\Delta(P$-ET) [mm/yr]
Nobre et al. (1991)	Am	fixed SST	+2.5	−643	−496	−147
Mylne and Rowntree (1992)	Am	z_0 unchanged, fixed SST	−0.11	−340	−179	−161
Henderson-Sellers et al. (1993)/ Pitman et al. (1993)	Am	mixed-layer ocean	+0.6	−588	−232	−356
Polcher and Laval (1994a)	Am	z_0 unchanged, fixed SST	+3.8	+394	−985	+1379
Polcher and Laval (1994b)	Am	fixed SST	+0.14	−186	−128	−58
McGuffie et al. (1995)	Am	mixed-layer ocean	+0.3	−437	−231	−206
Sud et al. (1996)	Am	fixed SST	+2.0	−540	−445	−95
Zhang et al. (1996)	Am	mixed-layer ocean	+0.3	−402	−222	−180
Lean and Rowntree (1997)	Am	fixed SST	+2.3	−157	−296	+139
Polcher and Laval (1994a)	Af	z_0 unchanged, fixed SST	+2.56	+88	−533	+621
Polcher and Laval (1994b)	Af	fixed SST	+0,03	−99	−95	−4
McGuffie et al. (1995)	Af	mixed-layer ocean	−0.09	−108	−89	−19
Zhang et al. (1996)	Af	mixed-layer ocean	−0.02	−63	−74	+11
Delire et al. (2001)	In	uncoupled	n.s.	−201	−201	0
Polcher and Laval (1994b)	In	fixed SST	−0.05	−281	−51	−230
Pitman et al. (1993)	SEA	mixed-layer ocean	−0.5	−19	−113	+94
McGuffie et al. (1995)	SEA	mixed-layer ocean	−0.69	−48	−128	+80
Zhang et al. (1996)	SEA	mixed-layer ocean	−0.2	−251	−138	−113
Sud et al. (1996)	Trop	fixed SST	+1.3	−266	−350	+84

Table 6. Sensitivities of temperature and CO_2 in comparison with Claussen et al. (2001), averaged over the final 150 years. In the case of tropical deforestation, the CO_2 anomaly was averaged over the final 30 years.

Experiment	DT	AT	DB	AB
Converted area in million km^2	−23.07	+10.52	−18.55	+26.72
CO_2 anomaly in ppm	+26.8	−4.0	+3.7	−6.5
CO_2 sensitivity in ppm/million km^2	−1.16	−0.38	−0.20	−0.24
CO_2 sensitivity in Claussen et al. (2001)	−0.83	−0.97	−0.60	−0.40
Temperature anomaly in K	+0.4	−0.06	−0.25	+0.26
Temperature sensitivity in K/million km^2	−0.017	−0.006	+0.013	+0.010
Temperature sensitivity in Claussen et al. (2001)	−0.010	−0.010	+0.015	+0.010

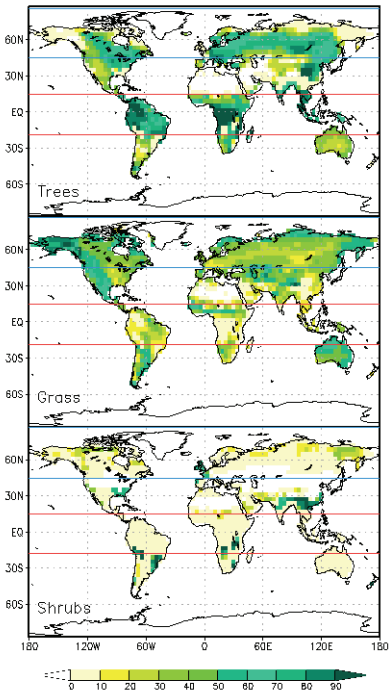

Fig. 1. Distribution of natural potential trees, grass and shrubs in the control experiment. Displayed is the fraction of each grid cell covered by the according vegetation. The blue and red lines contain the areas affected in the boreal and tropical experiments, respectively.

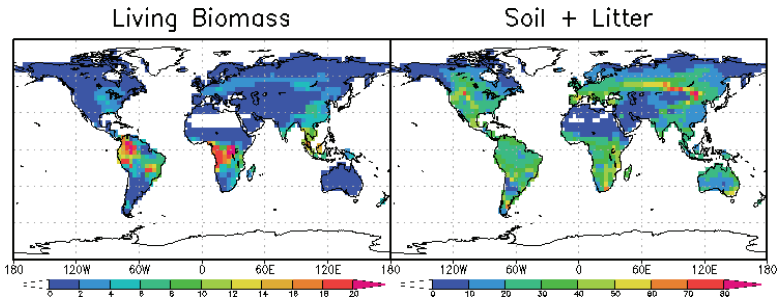

Fig. 2. Carbon storages in kg/m^2 for different pools of the control run.

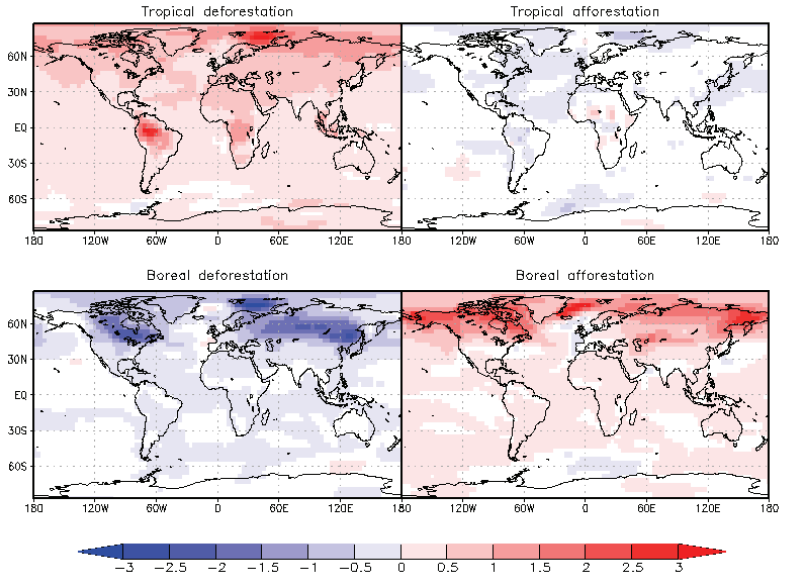

Fig. 3. Anomalies of 2m-temperature averaged over the final 200 years for each experiment. White areas show no significant changes according to a t-test with 95% significance.

421

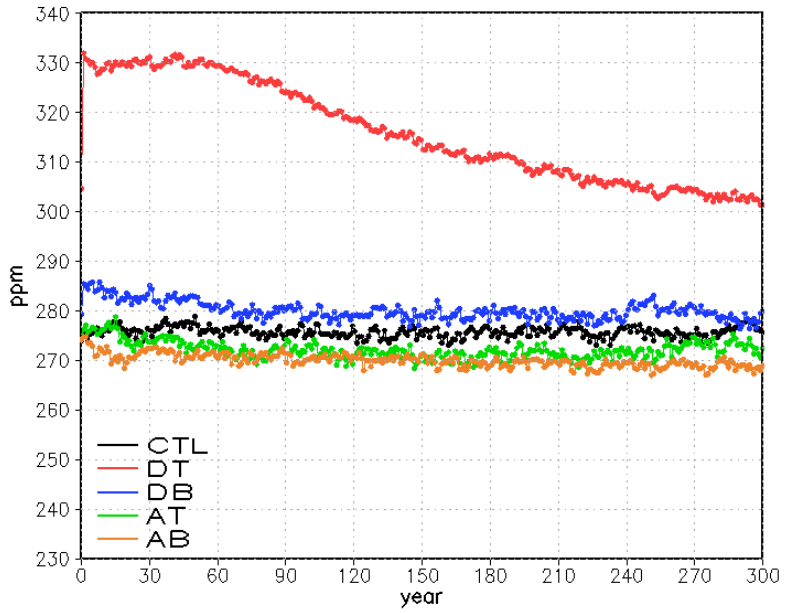

Fig. 4. Evolution of CO_2 concentration in each experiment.

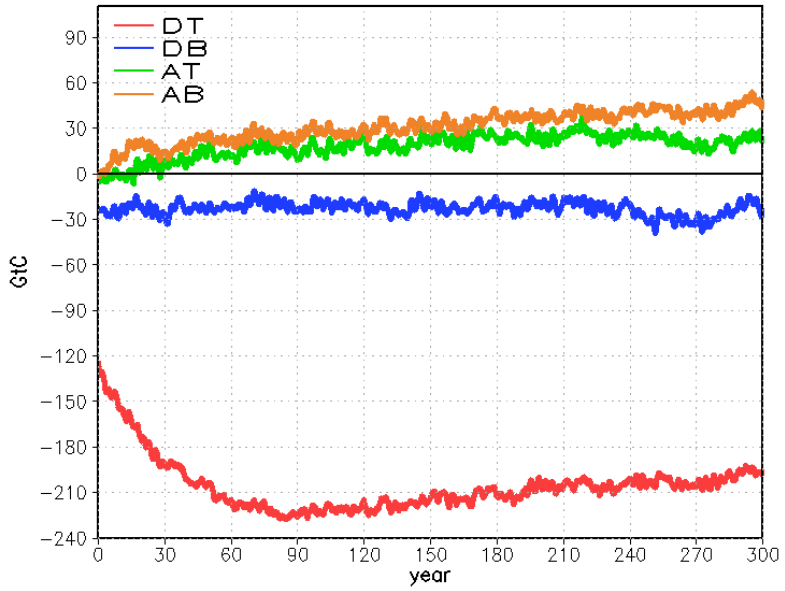

Fig. 5. Evolution of global terrestrial carbon in each experiment.

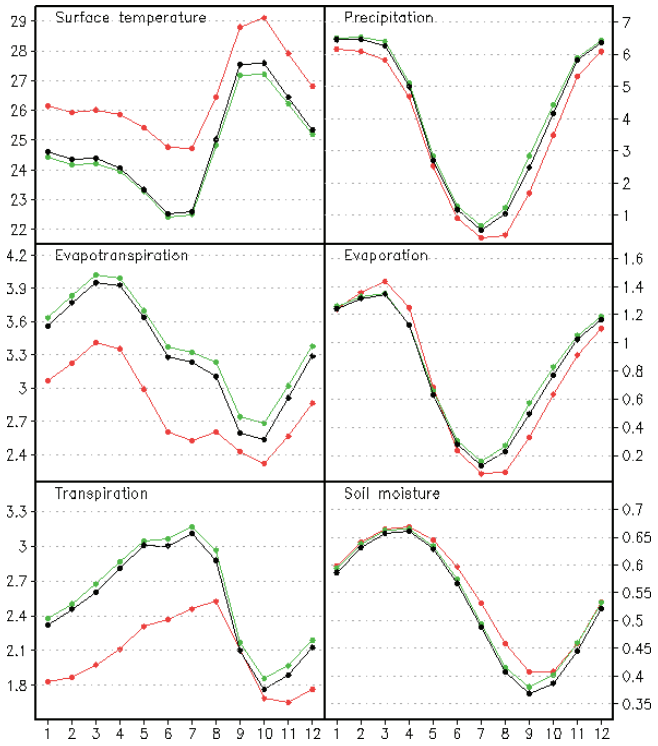

Fig. 6. Annual cycles averaged over the years 11 to 300 between 18.75° S and the equator in South America. Temperature is in °C, soil moisture in m, all fluxes in mm/day. Black: control climate, red: tropical deforestation, green: tropical afforestation.

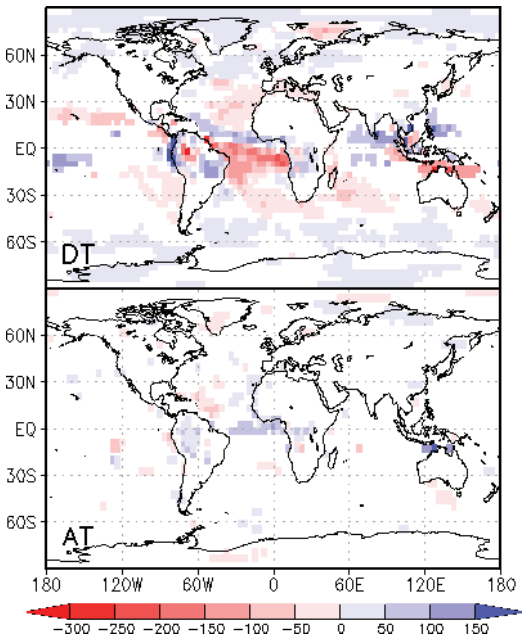

Fig. 7. Changes in annual mean moisture convergence in mm/yr, averaged over the years 11 to 300. White areas show no significant changes according to a t-test with 95% significance.

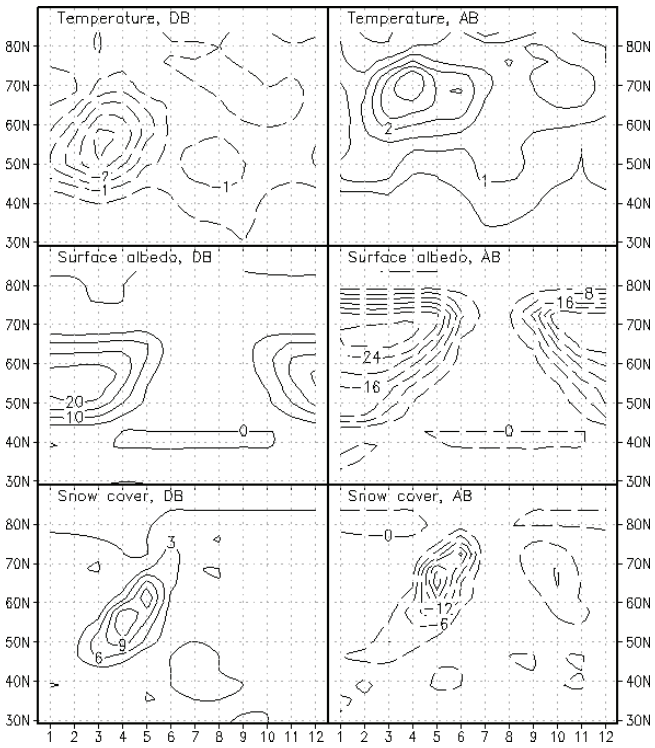

Fig. 8. Anomalies of surface temperature in K, albedo and snow cover in %, zonally averaged over all land cells during the final 200 years for boreal deforestation (left) and boreal afforestation (right).

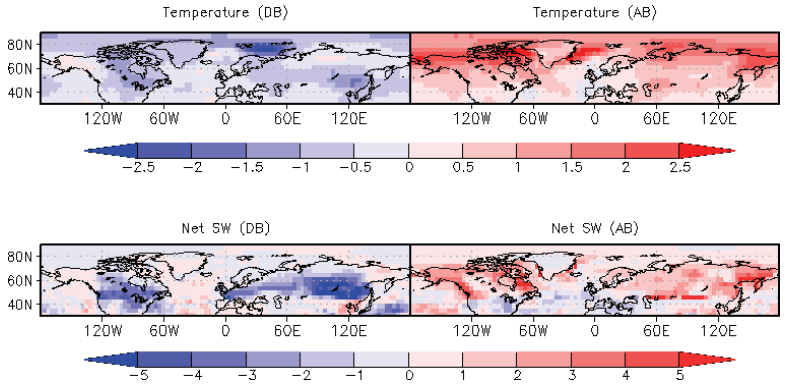

Fig. 9. Anomalies in 2m-temperature in ˚C and net short-wave radiation in W/m^2 at the surface for boreal autumn averaged over the final 200 years of the boreal deforestation (left) and boreal afforestation experiment (right).

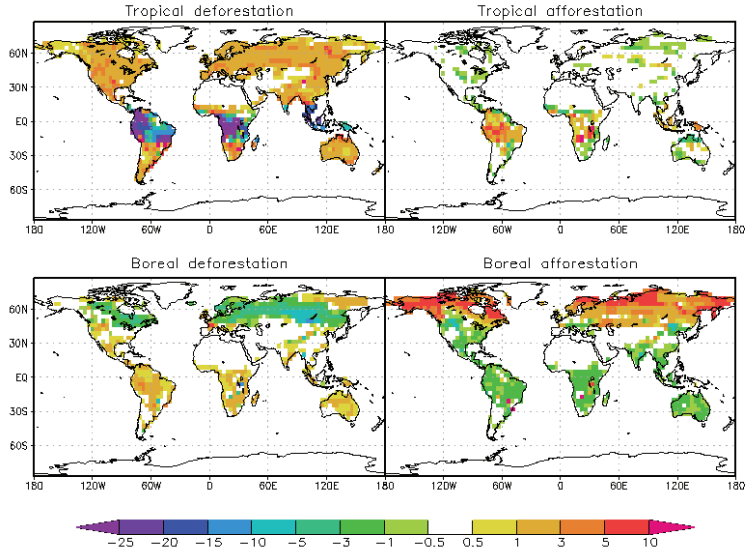

Fig. 10. Anomalies in total land carbon in kg/m^2 for each experiment, averaged over the final 10 years.